Spanish Journal of Agricultural Research
18 (4), e0210, 11 pages (2020)
eISSN: 2171-9292
https://doi.org/10.5424/sjar/2020184-15767
Instituto Nacional de Investigación y Tecnología Agraria y Alimentaria (INIA)

RESEARCH ARTICLE

OPEN ACCESS

Simulation of local head loss of drip-irrigation tape with integrated in-line emitters as a function of cross section

Yalin Wang (Wang, YL)[1], Xueliang Ju (Ju, XL)[2], Shijiang Zhu (Zhu, SJ)[1] and Meng Li (Li, M)[3]

[1] *College of Hydraulic & Environmental Engineering, China Three Gorges University, Hubei Yichang, China* [2] *Key Laboratory of Environmental Protection of State Grid Corporation of China, State Grid Shaanxi Electric Power Research Institute, Xi'an 710054, China* [3] *College of Biological & Pharmaceutical Sciences, China Three Gorges University, Hubei Yichang, China*

Abstract

Aim of study: To investigate how the cross section of a drip-irrigation tape affects local head loss.

Area of study: The work was carried out in the laboratory of Irrigation hydraulics, College of Water Conservancy and Environment, Three Gorges University, Yichang, Hubei province.

Material and methods: Tapes with six different wall thicknesses were studied experimentally to determine the relationship between cross-section deformation, wall thickness, and pressure. Based on the experimental results, we determined the factors that influence local head loss in drip-irrigation tapes by numerical simulation and dimensional analysis.

Main results: The cross-sectional shape of the drip-irrigation tape varied with pressure: under low pressure, the cross section was nearly elliptical. The cross-sectional shape of the tape strongly influenced the local head loss, which was inversely proportional to the 0.867th power of the flattening coefficient of the drip irrigation tape. We expressed the local head loss of a drip-irrigation tape equipped with integrated in-line emitters by considering the deformation of the cross section. Under the conditions used in this study, when the cross section is circular, the ratio of local head loss to frictional head loss was about 10% but, when the cross section is elliptical, this ratio increased to 15%.

Research highlights: The shape of the cross section of a drip-irrigation tape is nearly elliptical under low pressure. Local head loss is inversely proportional to the 0.867th power of that is the flatting coefficient of the drip-irrigation tape. Local head loss is about 1.5 times for elliptical tape than circular tape.

Additional key words: cross-section deformation; numerical simulation; dimensional analysis; micro-irrigation.

Authors' contributions: Conception, design and performed the experiments: ML, YLW. Acquisition, analysis, and interpretation of data: YLW, SJZ, XLJ. Drafting of the manuscript: YLW, ML. Contributed reagents/materials/analysis tools: YLW, SJZ, XLJ, ML. All authors read and approved the final manuscript.

Citation: Wang, YL; Ju, XL; Zhu, SJ, Li, M (2020). Simulation of local head loss of drip-irrigation tape with integrated in-line emitters as a function of cross section. Spanish Journal of Agricultural Research, Volume 18, Issue 4, e0210. https://doi.org/10.5424/sjar/2020184-15767

Received: 21 Sept 2019. **Accepted:** 20 Nov 2020.

Funding agencies/institutions	Project / Grant
Natural Science Foundation of Yichang, Hubei Province, China	1219073

Competing interests: The authors have declared that no competing interests exist.

Correspondence should be addressed to Meng Li: 1007326998@qq.com

Introduction

In the field of micro-irrigation, the widely used technique of low-pressure drip irrigation is highly efficient and saves energy. This technique is often implemented by using drip-irrigation tapes, which have thin walls. When transporting water at low pressure, the cross section of these tapes is often noncircular, and this deformation can affect the resistance to water flow. Therefore, to study the local head loss of emitters, we should consider how the deformation of the cross section of a drip-irrigation tape affects the performance of these tapes. Conventional trickle lateral head loss calculations are mostly based on the assumption of fixed circular lateral cross sections, which often prevents such methods of calculation from reflecting the real situation.

In recent years, numerous studies have focused on the head loss of various types of drip-irrigation pipes and drip-irrigation tapes (Bagarello *et al.*, 1997; Ferro, 1997; Provenzano & Pumo, 2004; Valiantzas, 2005; Demir

et al., 2007; Ravindra *et al.*, 2008; Yildirim, 2010; Tahir *et al*., 2021). The study of head loss in drip-irrigation tapes generally assumes a fixed circular lateral cross section, without considering how modifications to this shape affect head loss (Neto *et al.*, 2009). Exceptions to this trend include the work of Neto *et al.* (2014) and Provenzano *et al.* (2016), who studied the frictional head loss of soft, round, polyethylene pipe and considered how, when transporting water under high pressure, the cross section of the pipe affects the frictional head loss. However, these works do not explain the local head loss for pipes with elliptical cross sections. Due to the irregularity of the cross-sectional shape, the relationship between these deformations and local head loss is very complicated, which makes the study of the local head loss as a function of cross-sectional shape very challenging. One approach to the problem consists of numerical and dimensional analyses, which are widely used to study pipeline hydraulics (Demir *et al.*, 2007; Provenzano *et al.*, 2007; Yildirim, 2010; Wang *et al.*, 2018). Therefore, these two methods are used herein to study the local head loss of drip-irrigation tapes with varying cross section.

Based on experiments and numerical analysis of six different drip-irrigation tapes, the factors (including cross-section deformation) influencing local head loss are elucidated for drip-irrigation tapes with integrated in-line emitters. The local head loss of a drip-irrigation tape is numerically calculated for two conditions (circular and non-circular), and the results are compared experimental results to verify the accuracy and rationality of the hydraulic calculations.

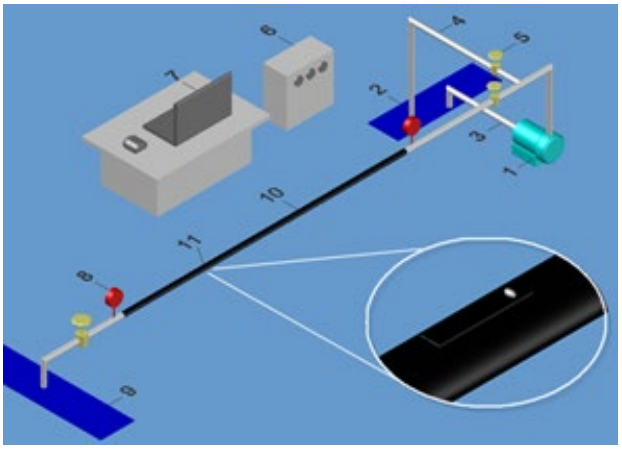

Figure 1. Sketch of experimental apparatus. 1, Pump. 2, Water tank. 3, Suction pipe. 4, Return pipe. 5, Valve. 6, Variable-frequency regulator. 7, Computer. 8, Manometer. 9, Return tank. 10, Drip-irrigation tape. 11, Blocked emitter.

Material and methods

Experimental setup

The experimental apparatus consisted of a water-supply device, pump, variable-frequency voltage regulator, drip-irrigation tape, pressure gauge, electronic scale, and electronic vernier calipers. The water tank was continuously supplied by an external water source. To ensure uniform discharge over the entire drip-irrigation tape, the emitters were sealed by viscose, as shown in Fig. 1. Six common commercial drip-irrigation tapes were used and were measured with an accuracy of 0.01 mm by using electronic calipers. These dimensions are listed in Table 1. The tapes had two forms: one was an inlaid-chip type with flaky in-line emitters, which accounts for five of the emitters studied herein, and the other (B4) was an inlaid-belt type with banded in-line emitters.

The inlet and outlet pressures of the drip-irrigation tape were measured with an accuracy of 0.1 kPa by using a pressure gauge. The lateral flow, which was calculated by using weighting methods, was controlled by adjusting the end valve. For discharge measurements, the vernier calipers were used to measure the horizontal and vertical diameters of the drip-irrigation tape to detect changes in the cross-sectional shape due to pressure variations. Based on the flow discharge, we calculated lateral flow velocity by using an electronic scale with an accuracy of 1 g. The water temperature was measured with an accuracy of 0.1 °C; the temperature range was 10.0~15.6 °C. After the tests, the data were divided into two groups: one group was used to verify the numerical simulation, and the other group was used to verify the analytical analysis (see below).

Numerical simulation and geometric model

The measured lateral discharge was taken as the initial inlet velocity. The lateral outlet was open to free flow into the ambient air. The simulation results varied by less than 1% when the number of grids in the numerical calculation exceeds 3.0×10^5. Thus, 3.0×10^5 grids satisfied the requirement that the results be independent of the number of grids. The final number of grids was $3.25\text{-}4.85\times10^5$ because we used a hybrid grid. The quality and momentum-conservation equations were available in the literature (Wang, 2016). Diffusion and convective terms are separated by using a central difference scheme and a second-order upwind scheme, respectively. The coupling calculation for velocity and pressure was based on the SIMPLEC algorithm. The no slip boundary condition was imposed on the lateral wall, and the flow near the lateral wall was simulated by using the standard wall function method. The Reynolds number was usually 10^4 at the laterals and the maximum Reynolds number at the lateral was 7.68×10^4 in this work, which is less than the smooth turbulence flow range of 10^5. The entire lateral flow evolved

Table 1. Dimensions of experimental drip irrigation tapes

Serial No.	Wall thickness [mm]	Outside diameter [mm]	Emitter spacing [m]	Emitter length [mm]	Emitter width [mm]	Emitter thickness [mm]
B1	0.47	16	0.3	33.6	6.1	2.5
B2	0.20	16	0.3	33.4	6.9	2.9
B3	0.23	16	0.3	8.5	5.9	2.8
B4	0.11	16	-	-	-	-
B5	0.21	16	0.3	33.5	6.1	3.0
B6	0.83	16	0.3	33.5	6.0	2.8

in the laminar, transition, and smooth turbulence flow zone. In addition, the transition flow zone was very small, so the transition flow was incorporated into the smooth turbulence zone. The laminar flow was not affected by the rough wall. Because of coverage by the viscous bottom layer, the turbulent core flow had no direct contact with the wall underneath the smooth turbulence flow, so the entire lateral flow was unaffected by the wall roughness. Thus, in the simulation settings, the parameter Roughness Height was set to zero because the surface of the lateral wall was uniform and flat, and the Roughness Constant was set to 0.5. Thus, the wall conditions in the simulation should reflect the experimental situation. Fig. 2 shows the grid and solid model.

The cross-sectional shape of a drip-irrigation tape changes as a function of pressure. Fig. 3 shows cross-sectional shapes of drip-irrigation tapes that correspond to different working conditions. The dimensions of the cross section are the horizontal inner diameter D_a and the vertical inner diameter D_b. For high pressure, the cross section of the drip-irrigation tape is approximately circular, as shown in Figs. 3d and 3e. For lower pressure, the cross section gradually changes to elliptical with flattening coefficient $\alpha = D_b / D_a$ that increases as the pressure decreases.

The outer diameter of the simulated drip-irrigation tapes were set to 12, 16, and 20 mm. We chose two common types of tapes: the inlaid-chip type and inlaid-belt type. The wall thickness range was 0.11 to 0.83 mm. For the length, thickness, and width of the emitters, we used 20, 33, 47, and 60 mm, 0.5, 1.3, 2.2, and 3 mm, and 3, 4.7, 6.3, and 8 mm, respectively. The emitters were separated by 0.3 m and the drip-irrigation tape was 5 m long. A total of 18 drip-irrigation tapes were set up at 20 and 30 °C, of which nine had circular cross sections and nine had elliptical cross sections. The ratio of vertical diameter to horizontal diameter was 0.28–0.7. Table 2 lists the cross-sectional dimensions of the drip-irrigation tapes.

Dimensional analysis and mathematical model

Dimensional analysis is commonly used in theoretical research and in hydraulics, especially to study complex

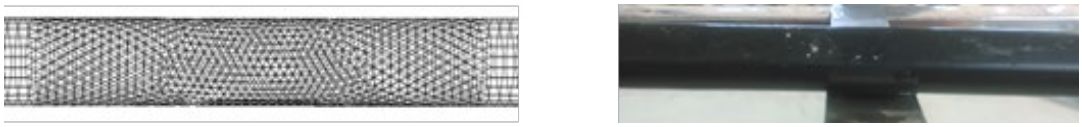

Figure 2. Mesh (left) and solid model (right).

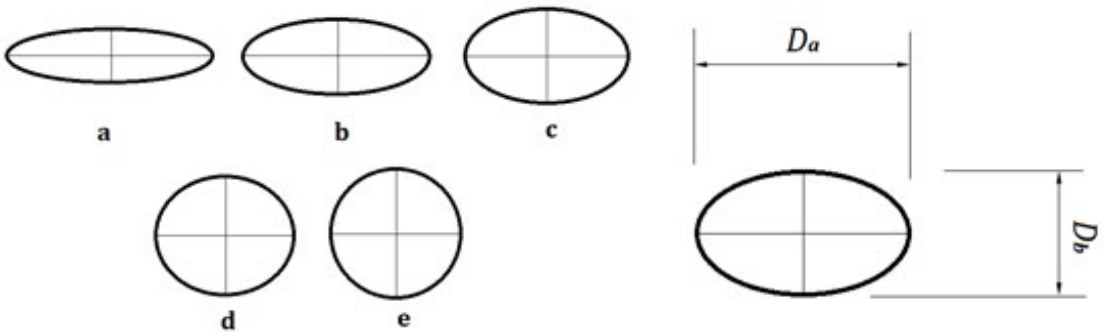

Figure 3. Cross-sectional shapes of drip-irrigation tape.

Table 2. Simulated drip irrigation tapes cross-section size

Serial No.	Outside diameter [mm]	Horizontal diameter [mm]	Vertical diameter [mm]	Serial number	Outside diameter [mm]	Horizontal diameter [mm]	Vertical diameter [mm]
Z1	16	15.6	15.6	Z10	20	19.2	19.2
Z2	16	17.1	13.0	Z11	20	21.0	16.0
Z3	16	21.1	6.0	Z12	20	25.6	8.0
Z4	16	15.6	15.6	Z13	12	11.8	11.8
Z5	16	17.1	13.0	Z14	12	12.8	10.0
Z6	16	21.1	6.0	Z15	12	14.0	8.0
Z7	20	19.2	19.2	Z16	12	11.8	11.8
Z8	20	21.0	16.0	Z17	12	12.8	10.0
Z9	20	25.6	8.0	Z18	12	14.0	8.0

factors, because it not only strengthens the theoretical results, but also reduces the research workload. Given that the factors affecting local head loss in drip irrigation tape are diverse and complex, we used dimensional analysis to derive a structural relationship for local head loss in drip-irrigation tape. According to experimental results, the local head loss h_j of drip-irrigation tape is a function of the emitter length E_l, emitter width E_h, and emitter thickness E_b, the cross-sectional major and minor axes D_a and D_b, respectively, and the velocity v, acceleration g due to gravity, and water-flow viscosity coefficient υ:

$$h_j = \varphi\left(E_l, E_h, E_b, D_a, D_b, v, g, \upsilon\right) \tag{1}$$

where SI units are used for all variables. According to the principle of dimensional analysis, we first found a number of fundamental physical quantities, and then constructed a dimensionless ratio by using the remaining physical quantities and the desired fundamental physical quantity:

$$\pi = \frac{x_{n-m}}{x_1^{\,a} x_2^{\,b} \cdots x_m^{\,r}} \tag{2}$$

where, x_1, x_2, …, x_m are the fundamental physical quantities in the physical process, *a, b*, …, *r* are the indexes of the fundamental physical quantities, n is the number of physical quantities contained in the physical process, and m is the number of fundamental physical quantities. In this paper, the horizontal diameter D_a and the flow velocity v were taken as the fundamental physical quantities. The remaining seven physical quantities and two fundamental physical quantities form the seven dimensionless π quantities shown in Table 3:

Substituting the dimensionless quantities of Table 3 into Eq. (1) gives

$$\frac{h_j}{D_a} = \varphi\left(\frac{E_l}{D_a}, \frac{E_h}{D_a}, \frac{E_b}{D_a}, \frac{D_b}{D_a}, \frac{gD_a}{v^2}, \frac{\upsilon}{D_a v}\right) \tag{3}$$

where h_j/D_a is the lateral head loss, E_l/D_a, E_h/D_a and E_b/D_a are the emitter dimensions, D_b/D_a is the lateral cross section, gD_a/v_2 is the Froude number and $/D_{av}$ is the Reynolds number.

Results

Analysis of deformation of drip irrigation

Consider a linear cross section for the drip-irrigation tapes (*i.e.*, the tape is collapsed), so no water flows through the tape, and the upper and lower pipe wall are

Table 3. Nondimensional terms of local head loss.

Pi term	Π_1	Π_2	Π_3	Π_4	Π_5	Π_6	Π_7
Expression	$\frac{h_j}{D_a}$	$\frac{E_l}{D_a}$	$\frac{E_h}{D_a}$	$\frac{E_b}{D_a}$	$\frac{D_b}{D_a}$	$\frac{gD_a}{v^2}$	$\frac{\upsilon}{D_a v}$

Table 4. Critical pressure for various tapes.

Drip-irrigation tape	Wall thickness [mm]	Critical pressure [m]
B1	0.47	2.70
B2	0.20	1.60
B3	0.23	2.20
B4	0.11	0.25
B5	0.21	0.70
B6	0.84	-

in contact with each other. When water flows through the tape, the upper and lower walls separate, and the cross section changes with water pressure. At low pressure, the tape does not fully expand, so the cross-sectional shape is a "flat" ellipse. Upon increasing the pressure, the cross section becomes more circular. In this paper, we used α as the flattening coefficient to quantify the flatness of the drip-irrigation tape. The expression for α is

$$\alpha = \frac{D_b}{D_a} \tag{4}$$

where D_b (D_a) is the vertical (horizontal) inner diameter of the drip-irrigation tape. A smaller (larger) α means that the drip-irrigation tape is flatter (rounder). The range of α is 0≤α≤1. The cross section corresponding to α = 0.9 is taken as the critical cross section between oval and circular; that is, the critical point where the cross-sectional shape changes qualitatively. The pressure corresponding to the critical cross section is called the critical pressure. For 0≤α≤0.9, the cross-sectional shape was nearly elliptical, and for 0.9≤α≤1, the cross-sectional shape was circular. Fig. 4 shows the flattening coefficient as a function of pressure for the six drip-irrigation tapes listed in Table 1.

Fig. 4 shows that the flattening coefficient increases with pressure for the six drip-irrigation tapes given in Table 1. The increase is rapid at low pressure, which indicates that the cross-sectional shape of the drip irrigation tape changes significantly in this range. When the pressure reaches the critical pressure, the increase becomes less rapid, indicating that the cross-sectional shape stabilizes. As the pressure increases further, the cross-sectional shape remains relatively constant as a function of pressure. The critical pressure for the various tapes is given in Table 4.

Numerical simulation and verification

To verify the reliability of the numerical model for the regimes of both circular and elliptical cross sections, the simulated results of the two numerical tapes were compared with the measured results. Tape B4 had the thinnest walls of the six experimental drip-irrigation tapes, so the cross-section of tape B4 under weak pressure expanded to round, and the measured results of B4 were used to verify the simulation results for a tape with circular cross

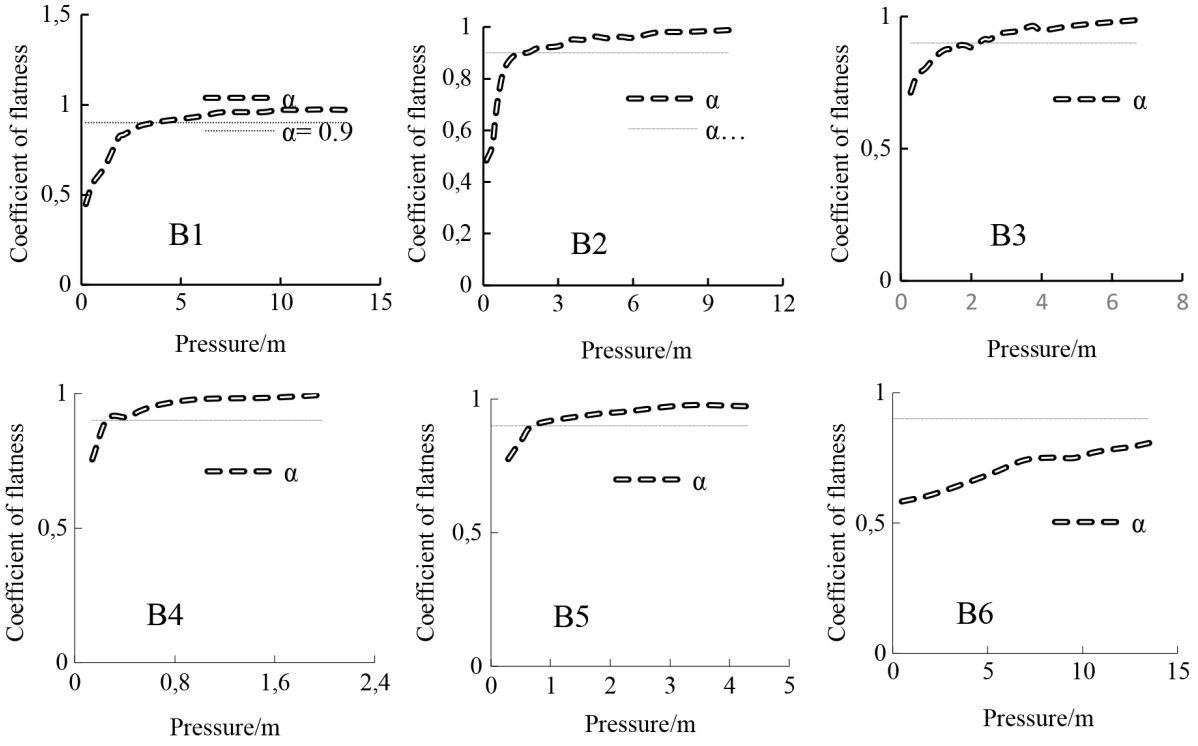

Figure 4. Flattening coefficient as a function of pressure for the six drip-irrigation tapes given in Table 1.

section. Tape B6 had the thickest walls so, even for larger pressure, the cross section remained flat. Thus, B6 was used to verify the simulation results for a tape with near-elliptical cross section. The remaining four sets of measured results were used to verify the fit.

Fig. 5 shows the simulated head loss as a function of measured head loss for tapes B4 and B6. The unity slope of these results indicates that the simulated head loss was consistent with the measured result. The average deviation between the measured and simulated results for tape B4 (B6) was 4.3% (8.5%). The larger average deviation for tape B6 is mainly attributed to the fact that tape B4 was circular, so the cross section varied only slightly (*i.e.*, over a relatively small range of flattening coefficient), and the simulated size of the tape was therefore always close to the actual size. The cross section of tape B6 was elliptical, so the measured cross section of tape B6 could vary more (*i.e.*, over a larger range of flattening coefficient). For tape B6, the measured head loss was slightly greater than the simulated head loss. The relative average deviation was satisfactory, so the simulation results are considered to accurately reflect the measured results.

Analysis of local head loss in drip irrigation

The numerical simulation of local head loss accurately reflects the measured local head loss in drip-irrigation tape. Therefore, we used the simulation results shown in Fig. 6 to analyze the drip-irrigation tape with 18 different cross sections. Fig. 6 shows the simulated local head loss as a function of water-flow velocity for 18 drip-irrigation tapes. The arguments of Eq. (3) were logarithmically processed, and the simulation results were linearly regressed to obtain the following expression of local head loss of drip-irrigation tapes:

$$\frac{h_j}{D_a} = 8.24\left(\frac{E_l}{D_a}\right)^{0.488}\left(\frac{E_h}{D_a}\right)^{1.23}\left(\frac{E_b}{D_a}\right)^{1.12}\left(\frac{D_b}{D_a}\right)^{-0.867}\left(\frac{gD_a}{v^2}\right)^{-0.874}\left(\frac{\upsilon}{D_a v}\right)^{0.043} \quad (5)$$

The correlation coefficient $R^2 = 0.92$. Table 5 lists the results of the regression analysis, which show that the Reynolds number in the 0.05 confidence interval fell within a probability of 0.58, so the impact of the Reynolds number on local head loss was not significant. The probabilities for the remaining factors were less than 0.01, so these factors were significant. Thus, the local head loss of drip-irrigation tape was related mainly to the

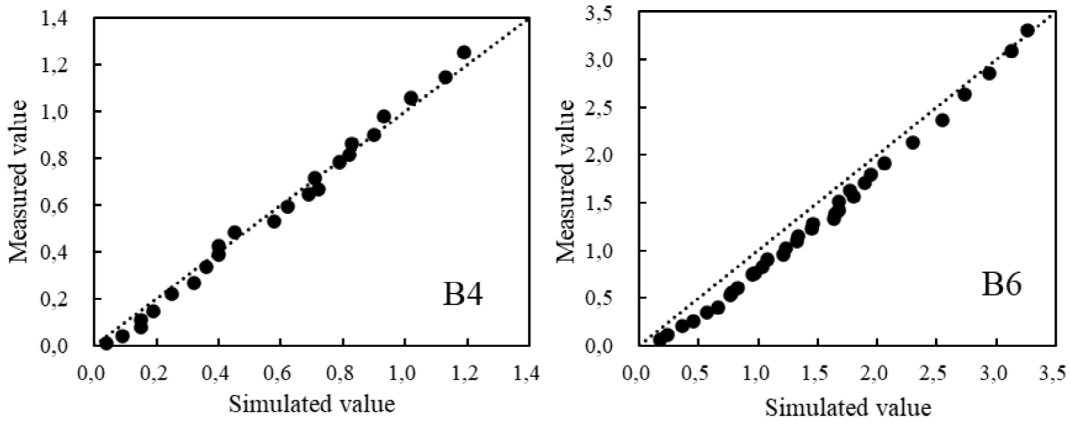

Figure 5. Simulated head loss plotted *vs* measured head loss for drip-irrigation tapes B4 and B6.

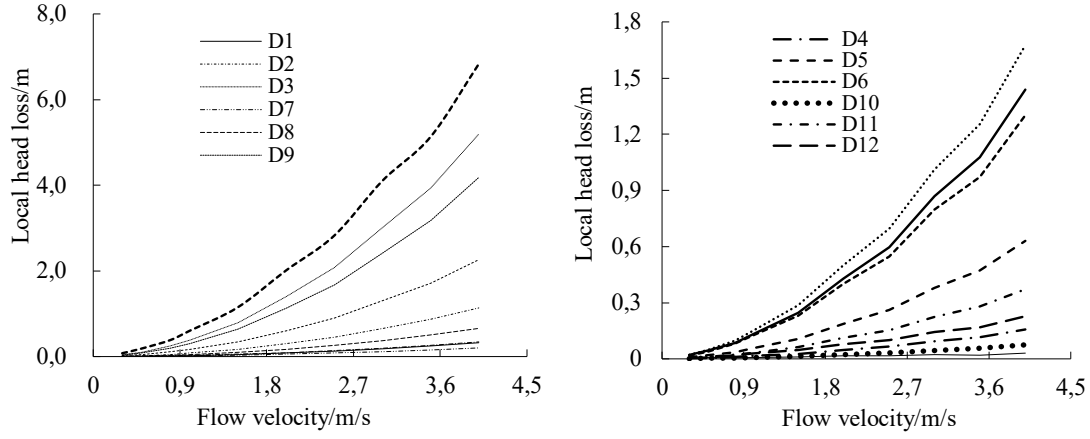

Figure 6. Simulated local head loss as a function of water-flow velocity for 18 drip-irrigation tapes.

Table 5. Results of multiple regression analysis for local head loss.

Pi terms	Exponent	Standard deviation	*t* test	*p*
Constant	2.11	0.73	2.89	<0.01
E_l/D_a	0.49	0.02	24.28	<0.01
E_h/D_a	1.23	0.10	12.21	<0.01
E_b/D_a	1.12	0.21	5.38	<0.01
D_b/D_a	−0.87	0.10	−8.32	<0.01
gD_a/v_2	−0.87	0.04	−21.61	<0.01
$\upsilon/D_a v$	0.04	0.08	0.55	0.58

shape of the emitter and the lateral diameter of the tape cross section.

We thus simplified Eq. (5), and using 9.8 m/s^2 for the acceleration due to gravity and a water-flow viscosity coefficient (for water at 20 °C) of 1.01×10^{-6}, obtained

$$h_j = 0.619E_l^{0.488}E_h^{1.23}E_b^{1.12}D_a^{-1.888}D_b^{-0.867}v^{1.7} \quad (6)$$

The lateral local head loss was related not only to the size of the emitter, but also to the lateral diameter and water-flow velocity. For a round cross section, the horizontal diameter equalled the vertical diameter ($D_a = D_b$), in which case we obtained

$$h_j = 0.619E_l^{0.488}E_h^{1.23}E_b^{1.12}D^{-2.755}v^{1.7} \quad (7)$$

where D is the diameter of the cross section.

To verify the accuracy of Eq. (6), we used it to calculate the local head loss for tapes B1, B2, B3, and B5 for both circular and elliptical cross sections. Under low pressure, the cross sections of these four drip-irrigation tapes were elliptical and their dimensions were compared against the simulation results for the near-elliptical condition. Under non-low-pressure conditions, the cross sections of the four drip-irrigation tapes were circular, so their dimensions were compared against the simulation results for circular tapes. Fig. 7 plots the simulation results for head loss versus the measured head loss. These results show that the simulation results for the four groups of drip-irrigation tape were consistent with the measured results. The average relative deviation for drip-irrigation tapes B1, B2, B3 and B5 was 8.3% 11.3%, 9.1% and 6.7%, respectively, and the overall average relative deviation of the four groups was about 10%.

Fig. 8 is the same as Fig. 7, but for the near-elliptical cross section. Again, the simulation results reflected the measured trend of local head loss of drip irrigation tapes, although a certain systematic deviation appeared, in particular for B3 and B5. The simulated head loss for B1 and B2 was consistent with the measured head loss (average relative deviations were 3.4% and 7.8%, respectively). The average relative deviation between the two was less than 10%. A larger average relative deviation was evident for tapes B3 and B5: 25.2% and 23.6%, respectively, and the average relative deviation between the two exceeded 20%.

Thus, for circular drip-irrigation tape, the simulated total head loss was consistent with measurements. For near-elliptical drip-irrigation tape, the simulated total head loss partially deviated from measurements, so the average relative deviation between the simulated and measured results was larger than for a circular drip-irrigation tape. This result is attributed to the cross section of the near-elliptical drip irrigation tape, which was approximated as elliptical, although its real shape was certainly irregular rather than elliptical. In some cases, this approximation assumes deviations from the actual shape of the cross section of the drip-irrigation tape, resulting in a greater deviation from the measured value. However, because the total average relative deviation of the four types of drip irrigation tape was 15%, we consider that the local head loss of each drip irrigation tape was satisfactorily approximated by Eq. (6).

To analyze the distribution of pressure and velocity in the drip-irrigation tape, we monitored the transverse and longitudinal sections of an emitter. The mechanism of the entire emitter was explored by monitoring the velocity and pressure distributions of the cross section. Fig. 9a shows a small inlet flow disturbance and a large export disturbance. The strongest disturbance upstream of the emitter was located in the area adjacent to the front end of the emitter. At the bottom of the lateral in this area appeared a large zone where the velocity was reduced in magnitude but not in direction, so the flow remained along the lateral direction. The strongest perturbation downstream of the emitter was near the end of the emitter. As can be seen from Fig. 9, the bottom of the lateral in this area was also a zone of low velocity, but the velocity was also negative, indicating that the downstream emitter caused reflux and a whirlpool. The range of the emitter head disturbance was small, whereas that of the end disturbance was large. The first section upstream of the emitter changed and the velocity distribution changed to the low-velocity regime. At the second section, however, the velocity distribution

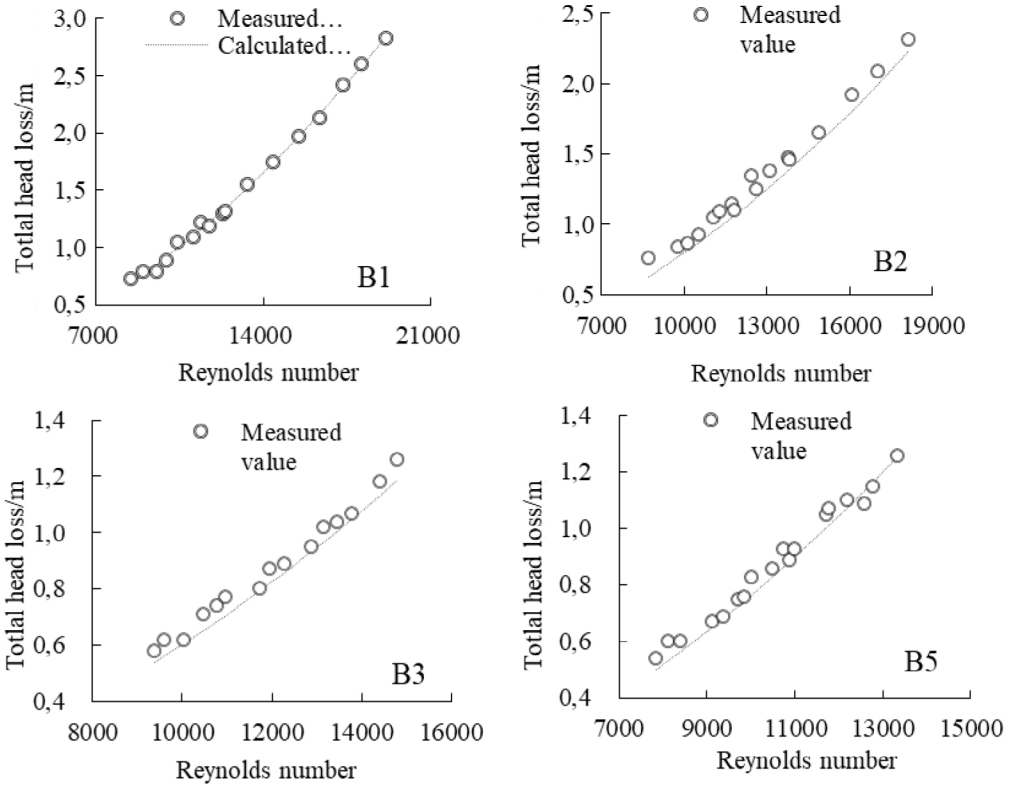

Figure 7. Estimated head loss as a function of measured head loss for drip-irrigation tape with round cross section.

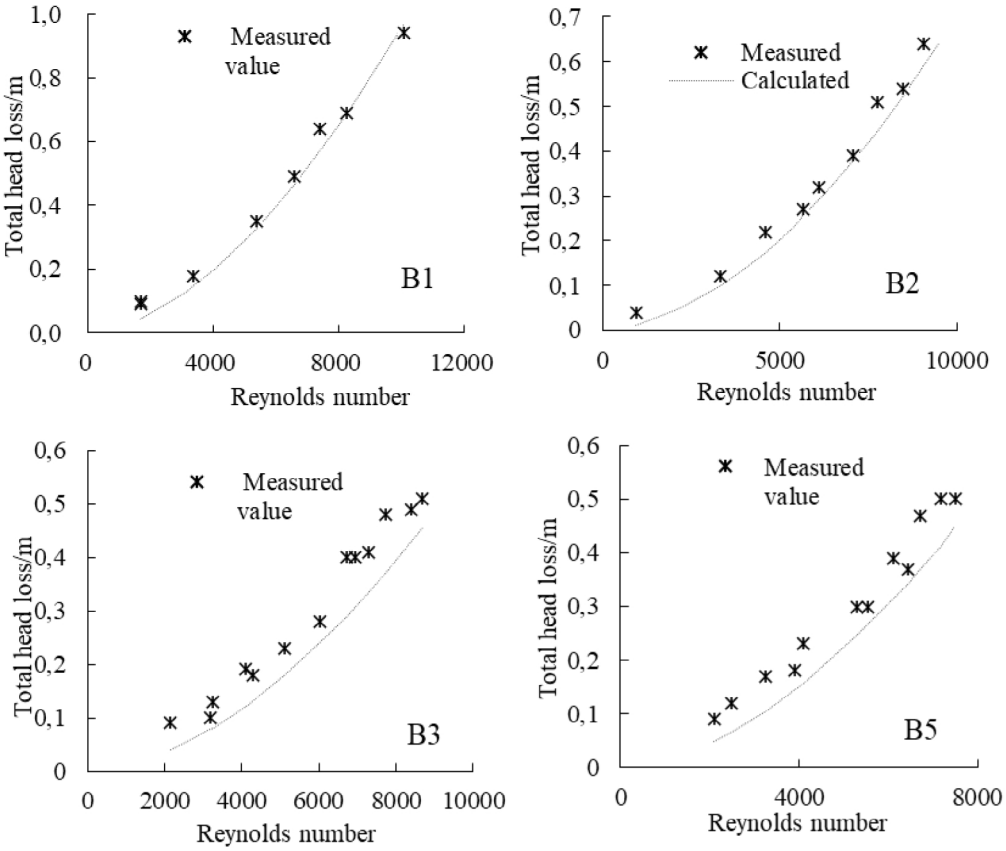

Figure 8. Estimated head loss as a function of measured head loss for drip-irrigation tape with elliptical cross section.

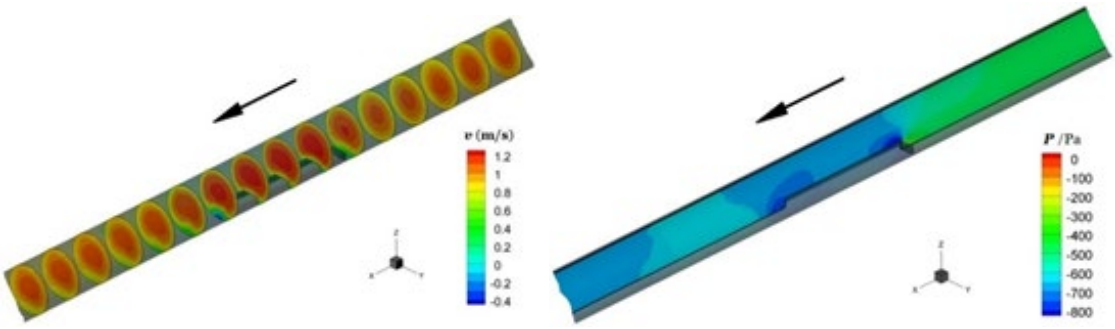

(a) **(b)**

Figure 9. Distribution of velocity (left) and pressure (right) of emitter unit.

returned to the axially symmetric distribution. At the first section downstream of the emitter, the velocity distribution changed to the low-velocity recirculation zone. The low-velocity zone continued to develop in the direction of the water flow. At the seventh section, the velocity distribution had not been restored to the axially symmetric distribution. The velocity distribution at the emitter was adjusted mainly downstream of the emitter. Fig. 9b shows that the low-pressure zone near the emitter occurred mainly in the top region of the tip of the emitter and in the tail region of the tip of the emitter, both of which were downstream of the cross-section deformation.

Case study

Given the expression (6) of the local head loss, we simulated a 60-m-long B1 φ16 drip-irrigation tape with integrated in-line emitters and calculate the local head loss in an actual engineering case study. The local head loss of the drip-irrigation tape was calculated separately for a round cross section and an elliptical cross section with flattening coefficient α = 0.76. We assumed uniform discharge from each emitter, and each emitter was numbered consecutively starting from the end of the drip-irrigation tape. The discharge was calculated from the end of the drip-irrigation tape by using the step-by-step method. In addition, the Reynolds number was calculated from the discharge. Reynolds numbers below 2000 corresponded to laminar flow, from 2000 to 3000 they corresponded to a transition from laminar to turbulent, and above 3000 they corresponded to turbulent flow. The friction head loss was calculated by using the Darcy-Weisbach formula, the Hagen formula, and the Blasius formula, and the head-loss coefficient for the transition section was fixed at 0.04 (Provenzano *et al.*, 2005; Palau-Salvador *et al.*, 2006; Zitterell *et al.*, 2014). The local head loss of the laminar-, transitional-, and turbulent-flow sections was calculated by using Eq. (6). In each section, friction head loss and local head loss were summed to obtain total head loss, and emitter discharge was set at 1, 2, and 4 L/h. The results appear in Table 6.

Table 6 showed that the local head loss and friction head loss of the drip-irrigation tapes varied as a function of cross-sectional shape. When the drip-irrigation tape had a flat cross section, the friction head loss and the local head loss were greater than when the tape had a circular cross section. The friction head loss increased slightly, whereas the local head loss increased by over 50%. The ratio of local head loss to friction head loss was 0.11–0.19 for elliptical tape, which was greater than the ratio 0.08–0.12 for circular tape. For both circular and elliptical

Table 6. Comparative analysis of head loss under different emitter flow in round drip irrigation tape and oval drip irrigation tape with a flatting coefficient α = 0.76.

Sectional shape	*q*[L/h]	*Re*	Δh_1[m]	Δh_2[m]	Δh [m]	$\Delta h_1/\Delta$	*hj* [m]	*hf* [m]	*hj*/*hf*
Round	1	22-4479	0.025	0.223	0.248	0.103	0.018	0.23	0.08
	2	45-8958	0.013	0.856	0.869	0.015	0.079	0.79	0.10
	4	90-17916	0.007	2.950	2.957	0.002	0.317	2.64	0.12
Oval	1	20-4084	0.027	0.246	0.273	0.100	0.026	0.25	0.11
	2	41-8169	0.014	0.967	0.980	0.014	0.131	0.85	0.15
	4	81-16339	0.007	3.384	3.391	0.002	0.553	2.84	0.19

cross sections and for laminar flow, the total head loss decreased with increasing emitter discharge. For turbulent flow, the total head loss increased strongly with increasing emitter discharge. In the design of drip-irrigation tapes, the local head loss was usually estimated to be 10% to 20% of the friction head loss. According to the results presented in Table 5, when the flow pressure gives a circular cross section, the ratio of local head loss to friction head loss was about 10%, but when the cross section was elliptical, the ratio of local head loss to friction head loss fell between 10% and 20%, so we used a median value of 15% to estimate this ratio.

Discussion

In the past, the local head loss at an emitter was calculated most often by assuming a circular pipe or a circular cross section. In this work, for low pressure, the cross section of the drip-irrigation tape was measured and found to be noncircular. The relationship between the local head loss and the shape of the cross section of the drip-irrigation tape was obtained by measuring the local head loss for tapes with differing cross-sectional shapes. According to Eqs. (1) and (5), the local head loss of the emitter was inversely proportional to 0.867α, where α is the flattening coefficient of the drip-irrigation tape. In other words, the flatter was the drip-irrigation tape, the larger was the local head loss (assuming other parameters were held constant). According to the results presented in Table 5, deforming the drip-irrigation tape strongly affects the local head loss of the emitter, which indicates that the effect on local head loss of the cross-sectional shape of drip-irrigation tape cannot be neglected.

This result is inconsistent with the results of previous studies on local head loss of drip-irrigation tape (Von Bernuth, 1990; Bagarello *et al.*, 1997; Provenzano & Pumo, 2004; Demir *et al.*, 2007). The reason that deformation of the tape cross section affects local head loss in the present study is that we consider low pressure, which means that some lateral flow occurs in the laminar regime. Most other studies satisfy the requirements of turbulent flow, so the calculations consider higher pressure and therefore give different results. The present results indicate that low-pressure and non-low-pressure conditions must be treated differently when calculating the head loss of drip-irrigation tape because these conditions lead to near-elliptical cross sections and circular cross sections, respectively. Given low-pressure conditions, the tape assumes a near-elliptical cross section, so the calculation must account for how deformation of the drip-irrigation tape affects the local head loss. In this case, the calculation given herein was appropriate, or it may be improved by including the proportion of local head loss calculated for a circular tape. According to the results presented herein, the local head loss for a near-elliptical cross section was about 50% more than that of a circular cross section. Therefore, given a near-elliptical cross section for a drip-irrigation tape, the local head loss should be increased by about 50%.

A positive correlation exists between local head loss and the size of the emitter in drip-irrigation tape: the emitter thickness had the strongest effect on local head loss, followed by the width and then by the length. This correlation indicates that the local head loss was mainly caused by the shape of the emitter whereas the length of the emitter had negligible impact. In addition, local head loss in drip-irrigation tape correlated negatively with the lateral cross section: it decreased with increasing lateral cross section of the drip-irrigation tape. The horizontal diameter of the drip-irrigation tape strongly influenced the local head loss, which indicates that the local head loss was more susceptible to the horizontal diameter. This result may be due to the greater emitter width, so that the change in the shape of the cross section caused by a change in the horizontal diameter of the drip-irrigation tape would be more noticeable, leading to a greater local head loss.

The inertia of the water caused the water flow to separate from the side wall when the lateral cross-sectional shape changed abruptly, which leads to negative pressure, and secondary flow occurred due to a lateral pressure difference. Numerous whirlpools appeared, violently mixing the water and converting mechanical energy into thermal energy. The energy input in the main stream quickly replenished the energy consumed by the vortex zone, and the energy transfer reached a dynamic equilibrium. Thus, the vortex movement, energy consumption, and local head loss continued to occur. When the drip-irrigation tape was flat, its cross-sectional area decreased, whereas the size of the emitter cross section was constant. Thus, the ratio of the area of the emitter to the area of the cross section increased, which is equivalent to increasing the size of the emitter and leads to an increase in the local head loss. Therefore, the local head loss for a flat drip-irrigation tape was greater than that for a drip-irrigation tape with circular cross section.

In conclusion, under low-pressure conditions, the non-circular cross section of the drip-irrigation tape can be calculated by using the elliptic approximation. The cross-sectional shape of the tape approaches a circle for thicker tape walls and for greater pressure. Although the simulated local head loss is slightly less than the measured local head loss, the relative deviations remain within an allowable range, so that the numerical simulation may be used to describe the real situation. The cross-sectional shape of the drip-irrigation tape clearly affects the local head loss of the drip-irrigation tape. When the drip-irrigation tape is flat, the local head loss in the tape is inversely proportional to 0.867th power of α, where α is the flatting coefficient of the drip-irrigation tape. For an actual

project, the low-pressure and non-low-pressure regimes must be treated separately to calculate the head loss of the drip-irrigation tape. For low pressure and a non-circular cross section of the drip-irrigation tape, the effect on head loss of cross-section deformation may be analyzed based on the examples given herein or by augmenting the results for a circular cross section by 50%. The experimental results show that some limitations apply regarding the type of drip-irrigation tape being analyzed. In addition, the conclusions above are based on the analysis of a drip-irrigation tape with integrated in-line emitters. Therefore, the precise calculation and microcosmic mechanism of the local head loss as a function of the precise cross section of a drip-irrigation tape remains to be done.

References

Bagarello V, Ferro V, Provenzano G, 1997. Evaluating pressure losses in drip-irrigation lines. J Irrig Drain Eng 123 (1): 1-7. https://doi.org/10.1061/(ASCE)0733-9437(1997)123:1(1)

Demir V, Yurdem H, Degirmencioglu A, 2007. Development of prediction models for friction losses in drip irrigation laterals equipped with integrated in-line and on-line emitters using dimensional analysis. Biosyst Eng 96 (4): 617-631. https://doi.org/10.1016/j.biosystemseng.2007.01.002

Ferro V, 1997. Applying hypothesis off self-similarity for flow-resistance law of small-diameter plastic pipe. J Irrig Drain Eng 123 (3): 175-179. https://doi.org/10.1061/(ASCE)0733-9437(1997)123:3(175)

Neto NO, Miranda JH, Frizzone JA, 2009. Local head loss of non-coaxial emitters inserted in polyethylene pipe. T ASABE 52 (3): 729-738. https://doi.org/10.13031/2013.27394

Neto OR, Botrel TA, Frizzone JA, 2014. Method for determining friction head loss along elastic pipes. Irrig Sci 32: 329-339. https://doi.org/10.1007/s00271-014-0431-7

Palau-Salvador G, Sanchis L, Gonzalez-Altozano P, Arviza-Valverde J, 2006. Real local losses estimation for on-line emitters using empirical and numerical procedures. J Irrig Drain Eng 132 (6): 522-530. https://doi.org/10.1061/(ASCE)0733-9437(2006)132:6(522)

Provenzano G, Pumo D, 2004. Experimental analysis of local pressure losses for microirrigation laterals. J Irrig Drain Eng 130 (4): 318-324. https://doi.org/10.1061/(ASCE)0733-9437(2004)130:4(318)

Provenzano G, Pumo D, Di Dio P, 2005. Simplified procedure to evaluate head losses in drip irrigation laterals. J Irrig Drain Eng 131 (4): 525-532. https://doi.org/10.1061/(ASCE)0733-9437(2005)131:6(525)

Provenzano G, Di Dio P, Palau-Salvador G, 2007. New computational fluid dynamic procedure to estimate friction and local losses in coextruded drip laterals. J Irrig Drain Eng 133 (6): 520-527. https://doi.org/10.1061/(ASCE)0733-9437(2007)133:6(520)

Provenzano G, Alagna V, Autovino D, Juarez JM, Rallo G, 2016. Analysis of geometrical relationships and friction losses in small-diameter lay-flat polyethylene pipes. J Irrig Drain Eng 142 (2): 1-9. https://doi.org/10.1061/(ASCE)IR.1943-4774.0000958

Ravindra VK, Rajesh PS, Pooran SM, 2008. Optimal design of pressurized irrigation subunit. J Irrig Drain Eng 134 (2): 137-146. https://doi.org/10.1061/(ASCE)0733-9437(2008)134:2(137)

Tahir M, Bo Z, Zeyuan L, Xiuzhi C, Yunkai L, 2021. Effects of phosphorus-fertigation on emitter clogging in drip irrigation system with saline water. Agr Water Manage 243: 106392. https://doi.org/10.1016/j.agwat.2020.106392

Valiantzas JD, 2005. Modified Hazen-Williams and Darcy-Weisbach equations for friction and local head losses along irrigation laterals. J Irrig Drain Eng 131 (4): 342-350. https://doi.org/10.1061/(ASCE)0733-9437(2005)131:4(342)

Von Bernuth RD, 1990. Simple and accurate friction loss equation for plastic pipe. J Irrig Drain Eng 116 (2): 294-298. https://doi.org/10.1061/(ASCE)0733-9437(1990)116:2(294)

Wang FJ, 2016. Research progress of computational model for rotating turbulent flow in fluid machinery. T Chin Soc Agr Machin 47 (2): 1-14.

Wang YL, Zhu DL, Zhang L, 2018. Simulation of local head loss in trickle lateral lines equipped with in-line emitters based on dimensional analysis. Irrig Drain 67: 572-581. https://doi.org/10.1002/ird.2273

Yildirim G, 2010. Total energy loss assessment for trickle lateral lines equipped with integrated in-line and on-line emitters. Irrig Sci 28 (4): 341-352. https://doi.org/10.1007/s00271-009-0197-5

Zitterell DB, Frizzone JA, Rettore Neto O, 2014. Dimensional analysis approach to estimate local head losses in microirrigation connectors. Irrig Sci 32 (3): 169-179. https://doi.org/10.1007/s00271-013-0424-y